B1-Mapping for 3T Body Imaging

Z. Zhai[1], D. Foxall[1], G. DeMeester[1], M. Morich[1], J. Duraj[1]
[1]Philips Medical Systems, Cleveland, Ohio, United States

Introduction

Increased image intensity non-uniformity is a main concern for clinical 3T body imaging when compared with conventional 1.5T results. The cause is poor B_1-field uniformity due to electro-dynamic effects. Knowledge of the B_1-field spatial distribution inside a patient provides useful data to correct the problem and can lead to improved image quality. Here we present the results of B_1-field calculation made using the FDTD method for a loaded 3T quadrature body coil, and compare these with B_1-mapping in a volunteer.

Methods

A shielded 16-element band-pass quadrature body coil (QBC) was modeled at 128MHz/3T using the FDTD method [1]. The QBC has the mean diameter of 60cm and length of 40cm. Its RF shield has a diameter of 68cm and length of 1m. The XFDTD software package (Remcom, Inc., State College, PA) was used to model the QBC space with 5mm isotropic resolution. Copper strips and rods in the coil were modeled as conductors with conductivity $\sigma = 5.8\times10^7$S/m. Capacitors in the coil structure were modeled by assigning passive loads across the gaps opened at their locations. Quadrature feed was supplied by assigning two sinusoidal voltage sources (f =128MHz) at the center of the two coil rungs located at 225° and 315°. A heterogeneous male body model with 23 distinct types of tissues, also obtained from Remcom, Inc., was used for these calculations. Portions of the arms were removed from the original model to eliminate contacts between hands and the torso. Figure 1 shows the diagram of a 3T QBC loaded with the human body model (the RF shield is not depicted) and the centering of the abdomen. Steady-state electromagnetic solutions were recorded and the laboratory frame field components converted to the B_1^+-field in the rotating frame [3]. B_1-field mapping was conducted in a volunteer using the interleaved 3D steady state technique at an isotropic resolution of 3.75mm, with sequence timings TR1/TR2/TE equal to 25/125/5ms at a nominal flip angle of 75° [2]. The data reconstruction accounted for the sign of the signal ratio formed from complex image data so local flip angle can be measured over the extended range 0-180°.

Results

Validation of the method was conducted by comparison between the calculated $|B_1^+|$-field and measured B_1-maps for an elliptical torso phantom with dimensions $33\times18\times33$cm^3 (width × depth × length). Figure 2(a) shows a transverse spin-echo image of the phantom, where upper and lower regions exhibit loss of image intensity. Figure 2(b) shows the calculated $|B_1^+|$-field, suggesting that, the signal loss is due to a locally weak transmit $|B_1^+|$-field (and possibly to a weak $|B_1^-|$-field for signal reception [3]). Figure 2(c) is the measured B_1-map, which is consistent with the FDTD calculation. Both results are also consistent with earlier analytical solutions for elliptic geometry [4]. Calculation for a cylindrical phantom reveals a better $|B_1^+|$-field uniformity than for the elliptical phantom. The elliptical phantom results explain to some degree why image uniformity seems worse for slim patients at 3T.

In Figure 3, we show the normalized ($|B_1^+|/|B_1^+|_{ref}$) in transverse and sagittal slices of the heterogeneous body model and the volunteer, respectively. The $|B_1^+|_{ref}$ is the reference $|B_1^+|$-field determined from RF scaling used for imaging. Referring to Figure 3, the $|B_1^+|$-field in the outer boundary of human body model is close to, but not precisely the same as the volunteer. Outer boundary shape is a key factor in determining $|B_1^+|$-field distribution. It is noted the volunteer geometry does not precisely match the human body model. However, global similarities exist between the calculated B_1^+-field in the heterogeneous body model and the B_1-map in the volunteer. Regions of both higher and lower $|B_1^+|$-field have quite similar spatial distributions in both slice orientations. Our measured B_1-maps are, however, marred by motion artifacts due to respiration. Multiplexing the acquisition read out, employing thin-slab encoding, and signal averaging can all be used to reduce this problem.

Conclusions

The global similarity between the calculated $|B_1^+|$-field from a heterogeneous human body model and the B_1-map of a volunteer validates use of our modeling work for RF coil design and clinical applications. Our calculations for a loaded 3T body coil suggest that B_1^+-field uniformity is affected by the geometric boundary of the image object. Prior knowledge of the B_1^+-field distribution as a function of subject geometry can be extremely useful for potential corrective strategies, such as multi-channel transmit with variable amplitude and phase [5] and other methods, to improve 3T body image quality.

References

[1]. C. M. Collins, et. al, MRM 40:847-856 (1998); T. S. Ibrahim, et. al, Magn. Reson. Imag. 18: 835-843 (2000).
[2]. V. L Yarnykh, et. al, Proc. Intl. Soc. Mag. Reson. Med, 12, p194 (2004).
[3]. D. I. Hoult, Concepts Magn. Reson. 12(4): 173-187 (2000).
[4]. J.G. Sled & G.B. Pike, IEEE Trans. Med. Imaging, 17: 653-662, (1998).
[5]. T. S. Ibrahim, et. al, Magn. Reson. Imag. 19: 1339-1347 (2001).

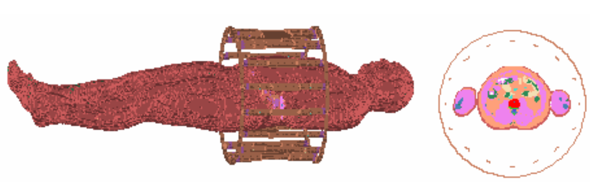

Fig. 1. Diagram of a human body model inside a 3T QBC (RF shield is not shown).

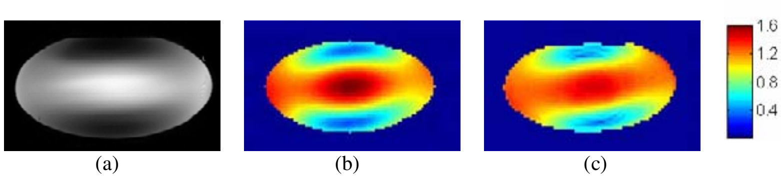

Fig. 2. The comparison between calculation and experimental B_1-map for an elliptical body phantom: (a) spin-echo transverse image; (b) FDTD calculated $|B_1^+|$-field; (c) experimental $|B_1^+|$-map.

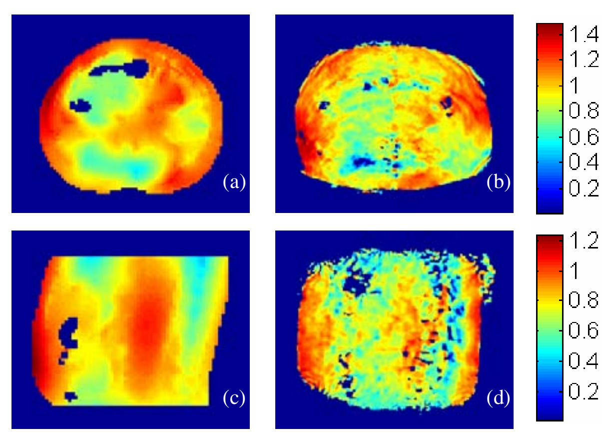

Fig 3. $|B_1^+|$-field distribution in transverse (a,b) and sagittal (c,d) slices for heterogeneous human model (a,c) and experimental B_1-map in a volunteer (b,d).